1960

The hyperfine frequency of potassium 39 in optically pumped gas cell frequency standards

Carr, John B.

THE HYPERFINE FREQUENCY OF POTASSIUM 39 IN OPTICALLY PUMPED GAS CELL FREQUENCY STANDARDS

JOHN B. CARR, JR.

UNITED STATES
NAVAL POSTGRADUATE SCHOOL

THESIS

THE HYPERFINE FREQUENCY OF
POTASSIUM 39 IN OPTICALLY PUMPED
GAS CELL FREQUENCY STANDARDS

by

John B. Carr, Jr.

Captain, United States Marine Corps

12ND P2238 (1-59)

THE HYPERFINE FREQUENCY OF POTASSIUM 39 IN OPTICALLY PUMPED GAS CELL FREQUENCY STANDARDS

* * * * *

John B. Carr, Jr.

THE HYPERFINE FREQUENCY OF POTASSIUM 39 IN OPTICALLY PUMPED GAS CELL FREQUENCY STANDARDS

by

John B. Carr, Jr.
//
Captain, United States Marine Corps

Submitted in partial fulfillment of
the requirements for the degree of

MASTER OF SCIENCE
IN
ENGINEERING ELECTRONICS

United States Naval Postgraduate School
Monterey, California

1960

THE HYPERFINE FREQUENCY OF POTASSIUM 39 IN OPTICALLY PUMPED GAS CELL FREQUENCY STANDARDS

by

John B. Carr, Jr.

This work is accepted as fulfilling
the thesis requirements for the degree of
MASTER OF SCIENCE
IN
ENGINEERING ELECTRONICS
from the
United States Naval Postgraduate School

ABSTRACT

Optically pumped gas cell frequency standards have been developed with long-term and short-term stabilities of one part in 10^{10}. The hyperfine transition frequency upon which the frequency standard is based is affected by certain factors which tend to shift the frequency. The effects of buffer gas pressure and temperature upon the hyperfine frequency of K^{39} were measured and recorded. The use of wall-coated absorption cells is discussed. The effect of the ambient magnetic field strength upon the hyperfine frequency was noted and the zero field hyperfine frequency for K^{39} was determined to be 461, 719, 685 $\pm$ 35 cps.

The study was conducted at Varian Associates, Palo Alto, California, during the period January to March, 1960.

The author wishes to express his gratitude to William E. Bell and Dr. Arnold L. Bloom of Varian Associates for their advice and assistance in this investigation. The guidance and encouragement given by Professor Carl E. Menneken of the United States Naval Postgraduate School are acknowledged with particular thanks.

TABLE OF CONTENTS

TABLE OF CONTENTS (Cont'd)

LIST OF ILLUSTRATIONS

1. Introduction

1-1. Frequency Stability Problem.

The development of many electronics systems of vital interest to the armed forces have been hampered by the non-availability of extremely stable frequency sources. MTI radar, navigation aids, and single sideband radio communications have a common requirement for precise frequency generation. A radio communication network utilizing oscillators so stable that negligible frequency drift would occur over extended periods of radio silence has immediate applications. The progress of electronic developments will have the effect of making the requirements for frequency stability more pressing and more stringent.

Among the developments in the expanding field of quantum electronics is the optically pumped gas cell frequency standard. This gas cell "clock" affords promise of the ultimate in frequency stability and deserves careful consideration.

The atomic transition which is the basis of the gas cell frequency standard is affected by factors which tend to "pull" the frequency. Certain factors also tend to broaden the line width of the signal or lower the Q of the system. This thesis is a systematic study of the above factors as applied to a system utilizing the most common isotope of potassium, K^{39}. Although similar studies of this type have been conducted using Cs^{133} [1] [2], Rb^{87} [3], and Na^{23} [2], this study of K^{39} is original. The theories involved are applicable to all alkali metal vapors.

1-2. Description of an Optically Pumped Gas Cell Frequency Standard.

A gas cell frequency standard utilizes the magnetic dipole transitions in the hyperfine levels of the ground state of the alkali metal atom as a frequency reference.

In the optically pumped system, the alkali metal atoms are "pumped" to an excited state by the energy contained in an incident light beam. When the excited state of the vapor is saturated, the light will pass through the cell with little attenuation. However, when the alkali metal atoms have been re-distributed throughout the lowest energy states, the intensity of the pumping beam is attenuated because of the energy withdrawn from the beam by the pumping process.

The re-distribution of alkali metal atom energies is obtained by radiating the vapor cell with radio frequency energy with a swept frequency whose range includes the transition frequency. At the instant of the dip in intensity of the light beam through the cell, which is detectable by use of a photocell, the frequency of the radio frequency signal generator corresponds to the atomic transition frequency.

After amplification, the signal from the photocell is processed by a servo system which extracts the phase information necessary to generate a correction signal to lock the radio frequency signal generator to the atomic transition frequency.

In its basic form, the optically pumped frequency standard consists of four units:

(1) a relatively stable radio frequency source.

(2) an alkali metal vapor absorption cell in a microwave cavity with associated optics.

(3) a pumping light source.

(4) a photocell amplifier and feedback servo-loop system.

The radio frequency source provides radio frequency energy at the atomic transition frequency with sufficient power to cause perturbation of the pumped energy states. This power requirement is in the order of one milliwatt. The oscillator must have sufficient short-term frequency stability to allow the servo system to track and lock on the transition frequency.

The absorption cell contains the alkali metal vapor plus an inert buffer gas to decrease the mean free paths of the alkali atoms or a paraffin wall coating. The alkali metal vapor when excited by the pumping light and then perturbed by the radio frequency energy provides the desired atomic transition. Alkali metal atoms are utilized because their single valence electron allows relatively easy excitation. The buffer gas or paraffin wall coating decreases the line width of the atomic transition by decreasing the disorientation effects acting on the excited states of the alkali metal atom.

Necessary conditions for the desired atomic transition are that the pumping light beam and the radio frequency magnetic field lines in the cavity be aligned parallel to the existing static magnetic field. Therefore, the cavity must be situated physically so that the magnetic field lines in the region of the absorption cell lie in the direction of the field lines of the static or earth's magnetic field. Also, the light beam from the lamp must pass through the cavity and cell along the same line. The cavity should resonate at the frequency of the desired atomic transition with a reasonably high Q.

The light source requires a lamp utilizing the same alkali metal vapor as contained in the absorption cell to provide light of the wavelength necessary for excitation of the atoms within the absorption cell. Because the lamp is the most serious source of noise in the system, its output should be carefully controlled.

Optics are used to increase the efficiency of the light system. Such optics may consist of lenses to collimate the pumping light through the absorption cell or lenses to focus the light from the cell onto the photocell. The optical system may also include interference filters and circular polarizers to provide light of the proper wavelength and polarization to enhance the pumping process.

1-3. Quantum Theory

The physical theory relating to the atomic transition of the optically pumped gas cell frequency standard is based upon the hyperfine splitting of the energy levels; i.e., the orientation of the spin of the valence electron of the alkali metal atom relative to the spin of the nucleus. The total energy of the atom is dependent upon this orientation. The two hyperfine levels of the ground state of the alkali metals correspond to the cases where the electron magnetic moment is aided by the smaller magnetic moment of the nucleus ($F = 2$) and that where the magnetic moments are opposing ($F = 1$).

The Zeeman effect concerns the further splitting of the hyperfine levels under the influence of a weak external magnetic field. The quantum number which represents the Zeeman sublevel, m_F, can take on any of $2F + 1$ values: $F, (F - 1), (F - 2), \ldots, 1, 0, -1, \ldots, -(F - 2), -(F - 1), -F$. Therefore, the $F = 1$ hyperfine level is split into three Zeeman sublevels: $m_F = 1, 0, -1$. The $F = 2$ level is split into five

sublevels: $m_F = 2, 1, 0, -1, -2$. The energy level diagram under the influence of a weak magnetic field is shown in Fig. 1-1.

It should be noted that the $m_F = 0$ energy levels lie parallel to each other. Therefore, the energy transition between these two states will be relatively independent of the strength of the external field. The field independence of this $\Delta F = 1$, $m_F = 0$ to $m_F = 0$, transition makes it ideally suited for a frequency reference.

In the transition, the relationship between frequency and energy is expressed as:

$$\Delta E = h f$$

where ΔE = energy level separation

h = Planck's constant

f = radiation frequency

In the case of K^{39}, the hyperfine frequency corresponding to the field independent transition is nominally 461.72 megacycles.

1-4. Optical Pumping Process.

In a system without some means of enhancement of the population difference of energy levels, the signal-to-noise ratio of the detection is poor because the amplitude of the signal is proportional to the unbalance of population of the energy levels between which the transition occurs.

At microwave frequencies, the unbalance in the population of the energy levels, $N_1 - N_2$, is given approximately by:

$$\frac{N_1 - N_2}{N} = \frac{h f}{2 k T}$$

where N = total number of atoms

h = Planck's constant

k = Boltzmann's constant

T = absolute temperature

f = transition frequency

At normal temperatures, this ratio is very small and the observable effect is extremely weak.[4]

Optical pumping is used to increase the population difference between energy levels. The energy of the pumping light excites the atoms to cause an abnormal concentration in certain energy levels.

The light absorption probabilities of the various Zeeman substates of the alkali metal atom are unequal. Also, the patterns of the absorption probabilities differ with different polarizations of the pumping light. The polarization of the pumping light restricts the Zeeman component of the light which will excite the atoms.

For magnetometer application, circularly polarized light is used for the pumping process. When using right circularly polarized D_1 radiation, the absorption probability of the substate, $F = 2$, $m_F = +2$, is zero. The other substates have finite absorption probabilities and therefore, may be excited to different states. From the excited states, the atoms relax back into the lower states with the transition probability of spontaneous emission. The relaxation process to the lower states is a random process, but the pumping process is controlled by the polarization of the light. The net result

is a concentration in the F = 2, m_F = + 2, state. The achievement of this population unbalance places the system in an emission state.[5]

For frequency standard application, an unbalance between the m_F = 0 substates is required in order to obtain the field independent transition. To achieve a population difference between the two m_F = 0 substates, a difference in light intensity exciting atoms out of these two levels is required, because the absorption probabilities are equal. The difference in intensity in the pumping light components is assumed to be achieved in the following process.

Light incident at the front of the absorption cell is absorbed and scattered separately by the alkali metal atoms in the two F levels. The rate of attenuation of the light components is proportional to the number of Zeeman sublevels in each F level; i.e., three and five for the lower and upper F levels respectively. This provides the necessary intensity difference at the rear of the absorption cell and produces a greater population in the upper states in this region.[6]

Therefore, to achieve an overpopulation of the F = 2, m_F = 0, substate, unpolarized light is used where the field independent transition is desired.

1-5. Transition Frequency Stability.

In an optically pumped gas cell frequency standard, the atomic transition of concern is the $\Delta F = 1$, $m_F = 0$ to $m_F = 0$, transition. The outstanding stability of this transition when subjected to the effects of electric and magnetic fields, pressure, temperature, etc., is the prime asset of the gas cell frequency standard. Standards with long-term and short-term stabilities of two parts in 10^{10} have been achieved.[7] An equivalent Q of over 3×10^8 have been obtained using optically pumped gas cell systems.[3]

The $\Delta F = 1$, $m_F = 0$ to $m_F = 0$, transition is termed the "field independent" transition because of its relative insensitivity to the effects of magnetic fields. The frequency dependence upon the magnetic field is given by the Breit-Rabi formula which is treated in Appendix I. In the case of K^{39}, this dependence is expressed as:

$$f = f_o + 8477\ H^2 \text{ cps}$$

where f_o = hyperfine frequency at zero field

H = magnetic field in gauss

This relationship is utilized to correct the experimental data for the strength of the ambient magnetic field in order to obtain the zero field hyperfine frequency.

The effect of diurnal variations in the strength of the earth's magnetic field upon the frequency stability of a K^{39} optically pumped gas cell frequency standard would be negligible because a field change of 1085 gamma is required to produce a frequency variation of one cycle. The diurnal variation is ordinarily in the range of 10 to 40 gamma. Magnetic storm variations rarely exceed 500 gamma.

The hyperfine frequency can be shifted slightly by interaction of the alkali metal atoms with those of any inert buffer gas in the absorption cell. This frequency shift due to the pressure of the buffer gas is the subject of Sections 2 and 3.

Because the above frequency shift is proportional to buffer gas pressure, the transition frequency can be affected indirectly by variations in the absorption cell temperature. This effect is discussed further in Section 5-2.

The transition is not seriously affected by electric fields or the Stark effect.

1-6. Transition Line Width

A limitation to the utility of the optically pumped gas cell frequency standard is the line width of the atomic transition which determines the effective Q of the system. Because the width of the transition line, when not restricted, can be expected to be of the order of several hundred kilocycles, this limitation can be quite serious when considering the design of a precise frequency standard.

Line broadening is caused by conditions which affect the environment surrounding the radiating atom or by interactions which disrupt the radiating process. The most serious factors which contribute to line broadening are:

(1) collisions of the alkali metal atoms with walls of the absorption cell.

(2) collisions of one alkali metal atom with another alkali metal atom.

Other line broadening factors of less concern listed in the order of the magnitude of their effect are:

(3) collisions of alkali atoms with buffer gas atoms.

(4) frequency modulation broadening.

(5) radio frequency power saturation effects.

(6) light intensity effects.

(7) Doppler effects.

(8) natural line breadth.

Collisions of alkali metal atoms with walls of the absorption cell constitute the most serious cause of line broadening. The radiation process of the alkali metal atom is terminated in the collision.

In a collision of two alkali metal atoms, the effects are evidenced which cause line broadening. The first case, which is negligible compared to the second, is a dipole-dipole interaction between the unpaired electron of each atom. The second effect is that of electron exchange. If two alkali metal atoms with oppositely directed electron spins collide, there is a probability of $\frac{1}{2}$ that the electrons interchange spin orientations. The result is equivalent to a spin inversion for each of the electrons and leads to relaxation of the excited energy states. The effect of electron exchange is to replace the atom's valence electron by one which is unpolarized and uncorrellated with the spin of the nucleus. Hence, after the exchange, the atoms are in a completely random spin state.

Of the less serious effects, that of alkali metal atom-buffer gas atom collisions is negligible for low pressures of the buffer gases. For the heavier buffer gases, the disorientation effect is noticeable for pressures greater than approximately 30 mm of Hg.

The effect of frequency modulation of the radio frequency signal generator is to cause line broadening. However, this factor can be minimized by reducing the magnitude of the sweep or by designing the system to eliminate the swept frequency signal. The magnitude of the line broadening is directly proportional to the magnitude of the sweep voltage.

Power saturation broadening results from a radio frequency magnetic resonance effect. The effect can be lessened by reducing the signal generator power output to a sufficiently low value. However, this also has the effect of reducing the magnitude of the detected signal.

Therefore, a satisfactory compromise must be reached between the two opposite effects. This observaton holds true in the case of light intensity broadening also, because the magnitudes of the line broadening and the detected signal are both proportional to light intensity.

Doppler effects are evidenced in the rapid diffusion of the atoms to regions within the cell of different radio frequency phase or direction. When the dimensions of the absorption cell are small compared to the wavelength of the radio frequency signal, there is negligible Doppler effect. The Doppler effect in this case is replaced by collision effects.

The natural line breadth is negligible compared to the other effects, being of the order of a fraction of a cycle per second. [87]

Without the presence of some mechanism to limit the relaxation effects of the collisions of alkali metal atoms with the cell walls and with other alkali metal atoms, the population inequalities achieved by pumping are reduced to the point where no signal can be detected. These collision effects have been successfully controlled by:

(1) inserting an inert buffer gas into the absorption cell to reduce the mean free path of the alkali metal atom, or

(2) coating the walls of the absorption cell with a paraffin which will not interact with the excited alkali metal atom.

Discussions of the buffer gas and the wall-coating techniques are included in Sections 2 and 4 respectively.

2. Buffer Gas

2-1. Theory of the Utilization of Buffer Gas

One effective means of reducing the line width of the atomic transition is to place a non-magnetic buffer gas in the cell along with the alkali metal. The mean free paths of the radiating atoms can be kept small by adjusting the buffer gas pressure. The proportion of collisions of the alkali metal atoms with the buffer gas atoms is increased as the relative number of alkali-alkali and alkali-wall collisions are reduced.

Collisions between an alkali atom and a buffer gas atom do not terminate the radiation process. The internal state of the radiating alkali atom is influenced only very weakly by this type of collision. [9]

The collisions of the alkali atoms with the buffer gas atoms will produce an increase in line width noticeable at high pressures of buffer gases. [10] The effects of these collisions, although weak individually, become the dominant cause of increased line width when the frequency of occurrence is increased by several orders of magnitude due to higher pressures.

Therefore, the addition of the buffer gas contributed to two opposing effects. It decreases the relaxation effects of the alkali-alkali and alkali-wall collisions but adds to the effect due to alkali-buffer collisions. An optimum buffer gas pressure exists at which the relaxation rate of the excited alkali atom is a minimum.

2-2. Effects of the Use of Buffer Gas

The addition of an inert buffer gas has three major effects upon the atomic transition:

(1) the line width is reduced.

(2) the signal-to-noise ratio is improved, and

(3) the center frequency of the transition is shifted slightly.

The first two effects are derived from the decrease in the collision effects which result in disorientation or relaxation processes.

In frequency standard application, the effect of most concern is the frequency shift in the field independent transition that is proportional to the pressure of the buffer gas.

2-3. Theory of Pressure Shift.

The hyperfine frequency of an alkali metal is the result of the interaction of the spin of the nucleus with that of the valence electron. During the collision between the alkali metal atom and the buffer gas atom, the valence electron wave is perturbed, modifying the energy of the system.

Pressure shift is defined as the shift in transition frequency that is proportional to the pressure of the buffer gas. Since the term, pressure shift, has achieved general usage in the field of optically pumped devices, it is used in the defined sense throughout this thesis.

The pressure shifts that have been measured in the alkali metals reveal a general trend of shifts toward the higher frequencies in the case of the lighter buffer gases and toward lower frequencies for the heavier gases.[1] [2] [3] Because these results include frequency shifts in both directions, the presence of exchange energies as well as dispersive forces are indicated. The exchange forces cause a higher frequency

shift. If active alone, the dispersion forces produce a frequency shift in the lower direction with all of the buffer gases.

The lower shifts can be attributed to the Van der Waals or long-range forces, which cause a downward displacement of the hyperfine energy states of the alkali metal atom as the buffer gas atom approaches.

The rare gas atom, commonly used as a buffer gas, consists entirely of closed electron shells and is relatively small. Conversely, the alkali valence electron is loosely bound. During the collision, the nucleus of the buffer gas atom will penetrate well inside the valence electron cloud, pulling it in with a corresponding increase of energy.[1] /11/ The hyperfine frequency is increased in proportion to the energy increase in accordance with the relationship:

$$\Delta E = h f$$

Therefore, the lighter buffer gases produce a greater positive frequency shift because the atoms are smaller and apparently succeed in a deeper and more effective penetration.

A linear relationship between the magnitude of the frequency shift and the buffer gas pressure exists. The result of increased buffer gas pressure is to increase the number of alkali-buffer atom collisions with a corresponding effect on the valence electron energies. Because of the linear relationship, pressure shift can be expressed distinctly as the slope of the plot of frequency versus buffer gas pressure. (See Fig. 3-9 and Table 3-1).

2-4. Predicted Pressure Shifts.

The pressure shifts of various buffer gases have been measured for gas cells of cesium, rubidium and sodium. The results of these measurements in terms of the frequency shift per unit of buffer gas pressure are listed in Table 2-1.

1. P.L. Bender, Comments on Dr. Fontana's Paper, published in the record of the Ann Arbor Conf. on Optical Pumping, June 15-18, 1959, pp. 107-108

Table 2-1. Pressure Shifts

Element	Cs^{133}		Rb^{87}	Na^{23}
Hyperfine frequency (f) (in mcs.)	9192		6834	1772
Pressure shift of buffer gas (Δf) (in cps/mm of Hg)				
He	+ 1050	+ 1750	+ 720	
H_2		+ 2000	+ 660	
N_2	+ 890	+ 950	+ 520	+ 80
N_e	+ 580	+ 700	+ 392	+ 58
Ar	- 190	- 300	- 51	0
Kr	- 1300	- 1300	- 580	
Xe		- 2400		
Reference	Bender (1)	Arditi (2)	Bender (3)	Arditi (2)

A reasonable correlation exists between the measured pressure shifts and the hyperfine frequencies of the alkali metals. The ratio of the pressure shift to the hyperfine frequency, $\Delta f/f$, demonstrates this relationship as is shown in Table 2-2.

Table 2-2 Ratio of Pressure Shift to Hyperfine Frequency (x 10^9)

Element	Cs^{133}		Rb^{87}	Na^{23}
Buffer Gas				
He	114	191	105	
H_2		218	97	
N_2	97	103	76	45
Ne	63	76	57	33
Ar	-21	-33	-8	0
Kr	-142	-142	-85	
Xe		-262		

In the ratio of pressure shift to the hyperfine frequency in Table 2-2, it is observed that this ratio decreases slightly with decreasing Z of the alkali metal. For a particular buffer gas, this ratio decreases from Cs^{133} to Rb^{87} to Na^{23}. In extrapolating this ratio for K^{39}, a value between those for Rb^{87} and Na^{23} is obtained.

Finally, the estimated pressure shift in cycles per second per millimeter of Hg, is obtained by multiplying the ratio, $\Delta f/f$, by the hyperfine frequency of K^{39}, which is roughly 462 megacycles. The results of these computations are shown in Table 2-3.

Table 2-3. Predicted Pressure Shifts for K^{39} (f = 462 mc.)

Buffer Gas	Δ f/f	Δ f
He	100	46 cps/mm of Hg
H_2	90	41.5
N_2	60	28
Ne	45	21
Ar	-5	-2.3
Kr	-70	-33
Xe	-130	-60

3. Pressure Shift Measurement.

3-1. Proposed measurement Procedure.

The frequency shifts due to the usually employed pressures (< 50 mm of Hg) of the non-magnetic buffer gases are very small in comparison with the hyperfine frequency. The maximum frequency shift is in the order of three kilocycles compared with the hyperfine frequency of 462 megacycles. The measurement procedure must be able to measure this L-band region transition frequency to within a few cycles of the correct value if the slope of the pressure shift curve is to be determined accurately.

A variety of measurement techniques are permitted by mounting two absorption cells side by side in the cavity so as to utilize the same light source and experience the same environment. Fig. 3-1 demonstrates this general arrangement. Three of the proposed techniques utilizing this arrangement are discussed below.

(I) Measurement technique utilizing two detection systems.

The simplest approach to the measurement of the frequency shift would be to establish the transition frequency of one selected gas cell as a frequency reference. The transition frequency of the selected cell would preferably be one corresponding closely to the zero pressure frequency. Therefore, the reference cell would contain a low pressure of a buffer gas which produces very little frequency shift, such as argon. The transition frequencies of the other cells using various buffer gases and pressures could be measured relative to the established reference frequency utilizing the frequency difference. The frequency differences should all lie in the audio frequency range, making them readily and accurately measureable.

The pressure shifts, i.e., the slopes of the plots of frequency versus buffer gas pressure, may be determined by this method. If the absolute frequencies of the data are desired, the transition frequency of the reference cell must be established using a frequency standard external to the gas cell system.

The proposed system would provide for simultaneous triggering of the transitions in the two different cells by amplitude modulating the radio frequency carrier with a single audio frequency. Fig. 3-2(a) shows how the carrier would be used to irradiate one cell while one of the sidebands would irradiate the other.

The light beams after leaving the two absorption cells would be detected and amplified in separate detection channels as shown in Fig. 3-2(b). The measurement would be accomplished by obtaining a signal in one channel using the carrier. After adjustment of the modulation frequency to obtain a signal in the other channel, the modulation frequency would be measured to obtain the frequency separation.

(II) Measurement technique utilizing sideband calibration.

The following approach utilizes the carrier and sideband technique also but eliminates the requirements for a second detection channel. This system would utilize a motor-drive helipot to tune the radio frequency signal source through the range of transition frequencies at a constant rate while recording the detected signals on a strip recorder. Fig. 3-3(a) is a block diagram of the system. When utilizing the carrier alone, the recording would be that of two signals separated by a distance equivalent to the frequency difference, as shown in Fig. 3-3(b). The strip recording would then be calibrated for distance on the strip versus frequency by amplitude modulating

the carrier and utilizing only one of the absorption cells. As shown in Fig. 3-3(c), the recording obtained by tuning the signal generator output through the frequency range in this case will be three signals representing the transition as it is triggered by the carrier and two sidebands as they are tuned through the transition frequency. The distance separating the carrier and sideband would be equivalent to the modulation frequency. A calibration would be obtained by equating the separation between the two signals in Fig. 3-3(b) to the separation between carrier and sidebands for a given audio frequency.

(III) Measurement technique utilizing individual measurements.

By inserting a shutter which would enable the selection of the individual cell desired of the two cells, the cells would be measured individually using an external frequency standard. However, one common cell could be utilized as a reference to check against variables in the system, such as drift in the external frequency standard. As shown in Fig. 3-4, this system requires less equipment than the previous two.

In evaluating the proposed systems, it is noted that all three have the advantage that the environments of the subject cell and the reference cell are identical with respect to both magnetic field and temperature.

In cases (I) and (II), the frequency separation could be read off of the dial of the audio oscillator readily and with reasonable accuracy.

The third case requires that all cells be measured individually. However, the measurement device need be calibrated for only one of the measurements, as the reference cell could be utilized to check against drift in the external standard.

The first prerequisite of the measurement procedure is the assembly of an optically pumped K^{39} gas cell frequency standard having sufficient stability, signal-to-noise ratio and narrow line width to permit an accurate determination of the transition frequencies in accordance with the prescribed technique.

In such a frequency standard, the radio frequency signal source should:

(1) exhibit extremely good short-term stability, i.e., in the order of a few parts in 10^8.

(2) deliver approximately five milliwatts of radio frequency power at the transition frequency.

(3) be tunable over a narrow band about the hyperfine frequency.

(4) be capable of a swept frequency output.

(5) provide for amplitude modulation.

A crystal-controlled oscillator can be obtained through careful engineering which will satisfy these requirements.

In order to attain a narrow line for enhanced accuracy of frequency measurement, the radio frequency power level must be restricted to a minimum. As mentioned previously, the effect of excessive power input to the resonant cavity is to broaden the line. However, the signal amplitude is directly proportional to the radio frequency power. Therefore, the problem of accurate frequency measurement resolves into that of maximizing the signal-to-noise ratio obtained from a weak radio frequency signal. The synchronous amplifier meets this requirement in addition to determining the line center accurately.

The synchronous amplifier is a correllation device which works on a phase detection principle utilizing the sweep frequency as the reference signal. A swept radio frequency signal is used because it enhances the amplitude of the detected signal and provides an alternating signal output which is less sensitive to noise and drift in the detection circuitry. A phase coherence exists between the sweep frequency and the detected light signal which permits a synchronous amplifier to determine the exact line center.

The lamp utilized should provide light of reasonably strong intensity with a minimum of noise and sweep frequency component. Where a 60 cps sweep frequency is utilized, any 60 cps component in the light tends to produce an erroneous result for the transition center frequency because the 60 cps sweep voltage is used as a reference signal for the synchronous amplifier.

The cavity should be resonant at the transition frequency of 462 megacycles with a Q of several hundred. The magnetic field lines within the volume occupied by the gas cell should be parallel to prevent any disorientation of the excited atoms due to magnetic field inhomogeniety or Doppler effect. At 462 megacycles, a reentrant type resonant cavity is preferable to a right-circular-cylindrical cavity operating in the TE_{011} mode because of the smaller size.

3-2. Pressure Shift Measurement.

The proposed procedure using two detection channels was rejected because of the extra equipment required to establish two identical detection channels. In particular, the second synchronous amplifier and a prism required to separate the two light beams were not readily available.

The proposed measurement technique utilizing sideband calibration was tested. However, the results when evaluated revealed that considerable discrepancies in the frequency separation measurements existed. The error in this procedure is believed to be due to the interaction of closely spaced signals in synchronous amplifier which have the effect of shifting the zero point or line center of the amplifier output.

The third method was the procedure utilized whereby the frequency of each cell was counted individually using the frequency of a reference cell to detect counter drift.

The reference cell chosen contained argon at a pressure of 1.75 mm of Hg as a buffer gas. Theoretically, argon should give a very small pressure shift. At a pressure of only 1.75 mm of Hg. the pressure shift would be negligible and the effects of temperature upon the transition frequency could also be neglected.

3-3. Characteristics of the Optically Pumped Gas Cell Frequency Standard Used.

The block diagram of Fig. 3-5 represents the frequency standard which was constructed for use in the pressure shift measurements. The major components of the system are described below.

(a) Radio frequency signal generator.

In order to provide a radio frequency signal source with adequate stability, a crystal-controlled oscillator was constructed. The signal generator circuit is shown schematically in Fig. 3-6.

The complete circuit consists of four stages. The first stage is a crystal oscillator circuit utilizing an overtone crystal with a frequency of 115.433 megacycles per second. The following two stages are doubler circuits which multiply the frequency to 230.866 and 461.732 megacycles per second respectively. A push-pull power amplifier stage with a power output of 5.0 milliwatts made up the final stage.

By varying the plate supply voltage of the crystal oscillator stage from 43 to 72 volts, the output frequency of the signal generator was pulled from 461,718,040 cps to 461,737,720 cps. Frequency control was maintained by use of a potentiometer in series with the power supply. A 90 volt dry cell battery as a power supply for this stage made possible a short-term stability of about four parts in 10^8 after warm up.

A filament transformer in series with the power supply superimposed a 60 cps sweep voltage upon the plate supply voltage. Because the magnitude of the sweep voltage has a significant effect upon the line width of the transition signal, the sweep voltage was adjusted with a Variac on the primary side of the transformer.

The construction of the signal generator provided for the monitoring of the 115 megacycles per second output of the crystal oscillator stage prior to doubling. This technique permitted the use of a Hewlett-Packard 524C frequency counter in conjunction with a Hewlett-Packard 525B frequency converter as the external frequency standard.

(b) Resonant cavity.

The resonant cavity used in the experiment was of the reentrant type tunable from 294 to 490 megacycles.

The reentrant cavity was in the form of a right-circular-cylinder with a tuning stub projected along the axis of the cylinder. Resonance occurs when the susceptance of the capacitance formed between the end of the tuning stub and the end plate is equal but opposite in sign to the susceptance of the effective inductance formed by the tuning stub, the end plates and the walls of the cavity. The design of the cavity is discussed in Appendix II.

For use in the optically pumped system, the cavity had windows to allow the passage of the light beam along a direction which was predominantly parallel to the radio frequency magnetic field within the region of the absorption cell. The magnetic field was circular about the axis of the cylindrical cavity. Therefore, a small perpendicular component is parallel to the light beam. The proper alignment of the cavity and optical system required that the radio frequency magnetic field and the pumping beam both lie parallel to the ambient magnetic field or H_o field.

The cavity was designed with a mount for insertion of two absorption cells side by side as shown in Fig. 3-1.

A probe was inserted into the center of one wall to provide for coupling radio frequency energy into the cavity. Diametrically opposite on the other side, a coupling loop was installed to allow sampling of the energy by a radio frequency power monitor.

The operating temperature for the potassium vapor cell is $70^{\circ} \pm 10^{\circ}C$. Two 100-watt Electrothermal heating tapes wrapped around the cylinder walls above and below the windows provided the necessary heating. The temperature, measured by an immersion type thermometer, was controlled by means of a Variac.

(c) Lamp.

The potassium lamp used was an electrodeless type excited by the inductive field of a 100 megacycle oscillator. The lamp bulb was of ordinary pyrex internally coated with potassium [illegible] and filled with natural potassium and krypton buffer gas at a pressure of 2.2 mm of Hg. Potassium 39 occurs as 93.2% of natural potassium. The buffer gas kept the lamp intensity from becoming temperature sensitive.

To obtain a constant, ripple-free source of pumping light, the 100 megacycle oscillator was driven by a well-regulated constant-current source, which provided 22-26 milliamperes of direct current. The filament power to the oscillator tubes was furnished by a storage battery to eliminate any 60 cps component in the light.

The lamp furnished a high light output with low noise. The lamp body was engineered to provide a constant source of heat to the lamp. To prevent variations in light intensity due to temperature variations, the entire lamp and oscillator assembly was inserted in a

glass container.

A warm-up period of approximately thirty minutes was necessary to allow the lamp and lamp body to achieve temperature stability and a stable operating condition.

(d) Synchronous amplifier.

The synchronous amplifier functions on a correlation principle integrating over the output of the photocell to obtain maximum signal. Using the sweep voltage to the radio frequency signal generator as a reference, the synchronous amplifier also determines when the signal generator frequency coincides with the transition frequency of the absorption cell by means of phase information carried in the detected light signal.

The schematic for the circuit of the synchronous amplifier is shown in Fig. 3-7. Every half cycle, the reference signal switches a chopper to reverse the polarity of the input signal to the integrating circuit. Hence, the input signal is added over one half-cycle and subtracted over the other.

When the center frequency of the signal generator is slowly varied through the transition in one direction, the synchronous detector output appears as shown in Fig. 3-8. The output signal increases as the transition frequency is approached, goes to zero at the time of coincidence, and increases in opposite polarity as the transition frequency is passed. The slope of the signal is seen to be very steep at the point of the transition which furnishes a sensitive accurate indication of the transition center frequency.

(e) Photocell and amplifiers.

In lieu of the standard vacuum tube photocell, a Hoffman type 2A silicon solar cell was utilized as the light sensitive element. The spectral response of the solar cell extends from 4000 Å to 11,500 Å with the peak near 8000 Å. This response is ideally suited to potassium resonance radiation, the two D lines being 7664 Å and 7699 Å. Although somewhat less sensitive than the standard photocell tube, the solar cell has two decisive advantages in being more compact and in not requiring an external power supply.

The solar cell was mounted directly on a transistor preamplifier. The preamplifier circuit consisted of two amplifier stages followed by an emitter follower stage. The overall gain of the preamplifier was 1000-1400, depending upon the condition of the battery.

The preamplifier was followed in the circuit by a Burr-Brown Model 110 Variable Gain AC Amplifier, a highly stable transistorized two stage feedback amplifier preceded by a set of impedance converting circuits. The gain of this amplifier was adjusted so that the overall gain through both the preamplifier and the amplifier was in the order of 50,000.

The efficiency of the optical system was enhanced by the utilization of a condensing lens following the gas cell to focus the light beam upon the solar cell. The placement of the lens following the gas cell increases the light signal without contributing to line-broadening.

(f) Gas cells.

The gas cells utilized in the project were made of laboratory quality Corning 7740 pyrex in the form of cylinders two inches in diameter and three inches in height.

The mount in the reentrant cavity held two of the cells side by side in a position such that the axis of the cylindrical cell was parallel to the light beam.

The distribution of buffer gas pressures necessary for the study was obtained by filling individual cells to the pressures desired. The absorption cells were filled by the following process. First, the cell was placed on a vacuum system which achieved a vacuum of approximately 10^{-6} mm of Hg. A small amount of natural potassium was then forced into the cell. A spectral grade inert buffer gas was inserted into the system and the cell was sealed off after achieving the desired buffer gas pressure.

Thirteen absorption cells containing buffer gases at the filling pressures listed below were utilized in the measurements.

Buffer Gas	Pressure (in mm of Hg)
He	2
	10.5
	28
	49
H_2	10
	29

Buffer Gas	Pressure (in mm of Hg) (cont'd)
Ne	10
	24.5
	35
Ar	1.75
	10
	30
Kr	11

3-4. Filling Pressure Accuracy.

The accuracy of the filling pressure of the buffer gas was limited by the filling techniques and the equipment available for making the cells. For this reason, a probable error of buffer gas pressure of ± 0.5 mm of Hg is assumed for all cells with the exception of those discussed below.

In the case of the two cells containing molecular hydrogen as the buffer gas, the filling technique was particularly difficult. The pressure of the hydrogen was achieved and maintained by heating a hydrogen compound which made the pressure difficult to regulate. Therefore, the exact pressure at the instant of sealing off the cell is subject to some uncertainty. In addition, the hydrogen when heated will react with the potassium to form potassium hydride, resulting in a lower buffer gas pressure. Since the tip of the cell must be heated in sealing off, this reaction probably occurs to an unknown extent. Due to this pressure accuracy limitation, a probable

error in the buffer gas pressure of ± 1.5 mm of Hg was assumed and only two H_2 cells were utilized in the measurements.

The cell containing potassium with a buffer gas of helium at 2 mm of Hg pressure was used in other experiments in which an electrical arc was developed in the cell on several occasions. An uncertainty exists as to the gas pressure resulting from this treatment and this cell was assigned a probable error of ± 1.5 mm of Hg.

3-5. Frequency Counter Accuracy.

A Hewlett-Packard 524C frequency counter in conjunction with a Hewlett-Packard 525B frequency converter were used to measure the transition frequencies.

The construction of the radio frequency signal source permitted the measurement of the frequency output of the crystal oscillator stage prior to multiplication. At that frequency level, the frequency falls within the range of the above instruments. The measured frequency was multiplied by a factor of four to obtain the output frequency of the signal generator.

Because the output level of the crystal oscillator stage was marginal in respect to the minimum trigger voltage of the counter, a Hewlett-Packard 460A wideband amplifier was used to amplify the input signal to insure against spurious counts.

The counter was placed in the circuit and left in continuous operation for a minimum of three hours prior to conducting any measurements.

Immediately following the measurements, the counter utilized was checked against two rubidium optically pumped gas cell frequency standards. The two rubidium clocks have been calibrated

against the cesium beam standard at Fort Monmouth. As a result of these checks, the frequency readings of the counter were determined to be 10 cycles per second low in the 462 megacycles per second region. The data was corrected by adding 10 cycles per second to cancel the counter error.

3-6. Measurement corrections.

In addition to the correction for the frequency counter accuracy of (+) 10 cps discussed in the previous section, the frequencies measured should be corrected to remove the effect of the ambient magnetic field.

The magnitude of the magnetic field was measured to be 0.51 gauss by means of a technique discussed in Appendix III. Substituting this value for H in the Breit-Rabi formula, a frequency correction of 2205 $\pm$ 3 cps is obtained. To obtain the zero field hyperfine frequency, the correction must be subtracted from the measured value.

The pressure of the buffer gas is dependent upon the temperature of the gas cell at the time of measurement. The temperature effects are discussed in detail in Section 5. The buffer gas pressures were corrected to reflect the change in temperature from the time of filling to the instant of measurement, which amounted to a pressure increase of 10.4%.

Because of variations in successive readings on any one cell, an experimental error of $\pm$ 20 cps was assumed for the measurement technique.

3-7. Pressure Shift Measurements.

The results of the measurements of the frequency shifts due to buffer gas pressure, after correction for the factors of counter accuracy, magnetic field strength and temperature, are plotted in Fig. 3-9.

Since the relationship between the frequency shift and buffer gas pressure is a linear one, the slopes of the plots express the pressure shift. In this form, the results are presented in Table 3-1.

Table 3-1

Buffer Gas	Pressure Shift (cps/mm Hg)
He	42.8 ± 4
H_2	35.6 ± 5
Ne	23.8 ± 2
Ar	-0.7 ± 1.0
Kr	-46.2 ± 5

3-8. Zero Field Hyperfine Frequency For K^{39}.

From Fig. 3-9, it is noted that all pressure shifts are linear and extrapolate to the same frequency at zero pressure. This fact lends considerable support to the accuracy of the results as the frequencies at zero pressure for all buffer gases should be the same regardless of the frequency-pressure relationship.

After correction to zero magnetic field strength and for counter error, the zero field hyperfine frequency for K^{39} was obtained from the point of zero pressure as:

$$f_o\ (K^{39}) = 461{,}719{,}685 \pm 35 \text{ cps}$$

This value should be compared with the previous value for the hyperfine frequency of 461,723 ± 10 kcs.[12] From the results of this work, it appears that measurements using the optical pumping technique are much more accurate and more precise than those obtained by previous methods.

3-9. Comments Upon Observed Signal Strengths.

The signal from the cell which contained the krypton as a buffer gas was weaker by an order of magnitude than the signals from the cells containing other buffer gases.

A possible explanation for the poor signal is that the krypton atom is a relatively large and therefore is easily deformed in a collision with a potassium atom. The deformation results in an interaction with the alkali vapor atom which tends to reduce the oscillating dipole moment of the atom. The overall effect is to cause relaxation at a rate so great that the effectiveness of the pumping is reduced to a relatively small value. The required population difference between the

$m_F = 0$ states cannot be maintained because the atoms relax back into lower states almost as rapidly as they are excited.[2]

Because krypton buffer gas cells invariably give relatively weak signals, its use in optically pumped gas cell systems is impractical. For this reason, only one krypton cell was measured. The purpose of this measurement was solely to demonstrate the large negative pressure shift characteristic.

The cell containing argon at a pressure of 30 mm of Hg also gave a very weak signal. The physical process which produces this effect is similar to that in krypton in that it is the result of an interaction between the alkali metal atom and the buffer gas atom during a collision. However, a distinction between the effects of the two gases lies in the more pronounced effect due to the larger krypton atom. The weak signal from the high pressure argon buffer resulted from the accumulation of lesser interactions over a greater number of collisions due to the greater pressure. This is borne out by the fact that the signals from a cell containing argon at only 10 mm of Hg were very strong.

3-10. Utilization of Combinations of Buffer Gases.

A buffer gas with a pressure shift of zero is very desirable for use in a gas cell frequency standard because the frequency variation that is indirectly due to changes of cell temperature is eliminated. Although argon is very good in this respect, none of the gases measured fulfill the requirement of zero pressure shift. However, both positive and negative shifts were observed which raises the possibility that combinations of buffer gases in proper proportions would give an

[2]Conversation with Dr. A.L.Bloom

overall zero pressure shift characteristic.

This technique has been utilized previously with other alkali metal vapors with considerable success.[1] [2] However, one case is recorded of a mixture of 75% Ar - 25% Ne in a Cs-[illegible] cell which gave no pressure shift for a cell temperature of 23°C. However, at higher temperatures, the shift was linear and negative, and at lower temperatures, the shift was linear and positive.[4]

Measurements utilizing mixtures of buffer gases in a K^{39} cell were not conducted because of the difficulty of making up such cells and the time available.

4. Wall-coated Cells.

4-1. Utilization of Wall-coated Cells.

Relaxation times are shortened most seriously by collisions of an alkali metal atom with the wall of the cell, this being the major cause of disorientation. This relaxation effect can be inhibited by coating the walls of the cell with an inert material which will not interact with the excited alkali metal atom.

The wall-coated cell does not reduce the number of collisions between one alkali metal atom and another. Theoretically, the narrowest lines should be attained by utilizing a wall-coated cell with a low pressure of buffer gas as this combination of techniques would suppress both of the serious collision effects.

Utilization of wall-coating has been previously reported. Experiments using eicosane, $C_{20}H_{42}$, a straight-chain saturated paraffin, as a wall coating have demonstrated that at least 600 wall collisions occur before appreciable disorientation of the spin takes place.[13] Some effects which indicated a possible chemical reaction between the rubidium and the eicosane at higher temperatures resulting in appreciably shortened relaxation times were observed.

Tests utilizing a cell lined with tetracontane, a straight-chain hydrocarbon of chemical composition $C_{40}H_{82}$, were less successful because of the experimental set-up. A reservoir of rubidium in the cell was exposed to collisions with the vapor. Therefore, the effectiveness of the wall coating could only be extrapolated. However, the relaxation time was increased by a factor of 12. This experiment also utilized a wall-coated cell in conjunction with neon buffer gas to obtain some extremely narrow line widths.[14]

The manufacture of a wall-coated cell is a very difficult process. The paraffin is heated and forced into the cell as a vapor. An even coating is obtained by cooling the cell walls to achieve condensation over the entire surface. Repeated heatings and coolings may be required to obtain a complete even covering. The potassium is then introduced. The correct technique requires that the potassium be deposited into the cell in a single globule. If the potassium is heated too much in the filling process, it will vaporize and spray into the cell condensing out in a layer covering the entire wall opposite the input tube. When this occurs, the potassium covering on the paraffin completely cancels its effectiveness, and the relaxation effect is increased to the point where no signal can be produced.

4-2. Results of Measurements Using Wall-coated Cells.

Measurements were made using two cells coated with dotriacontane, $C_{32}H_{66}$. One, a 2 x 3 inch cylinder, was newly prepared and the other, a one liter flask, was prepared for another experiment one year ago. Neither cell evidenced a significant pressure shift from the extrapolated zero pressure frequency nor did they show any temperature shift. A line width as narrow as 300 cps was observed with a signal-to-noise ratio, indicating that the linewidth in the absence of the broadening effects of excessive radio frequency power and pumping light intensity is probably considerably narrower.

The wall-coating when heated to 70°C produces a vapor pressure of the order of 10^{-6} mm of Hg. The straight-chain hydrocarbons have a tendency to produce a relatively strong negative frequency shift.[27]

However, due to the low vapor pressure, the measured frequency shift was negligible. The effect was so small that it could not be detected over the range of operating temperatures of the equipment. The transition frequencies of both of the wall-coated cells fell within experimental accuracy of the zero pressure hyperfine frequency of 461,719,685 $\pm$ 35 cps.

The $C_{32}H_{66}$ wall coating used has a melting point of 64°C, which prohibits its use in sodium cells which operate at temperatures of 120°C This effect in the case of potassium cells caused the paraffin to melt and form a pool in the lower portion of the cell. Although not observed, the liquid paraffin could possibly obstruct the light beam through the cell.

5. Temperature Effects.

5-1. Cell Operating Temperature.

The optimum cell temperature is determined by two factors:

(1) The temperature must be high enough to maintain a satisfactory vapor pressure of the alkali metal for utilization in the atomic transition process.

(2) The temperature of the cell imparts a kinetic energy to the alkali metal atoms. Excessive temperature results in increased velocities of the atoms with more disorientation-producing collisions. Therefore, too high a temperature will result in unacceptable relaxation effects.

The optimum temperature, giving the greatest signal-to-noise ratio, was measured to be 70°C. This corresponds to a potassium vapor pressure of 1.6×10^{-6} mm of Hg. [15] The operating range of temperatures extend approximately 15°C on either side of the optimum temperature; i.e., 70° ± 15°C.

5-2. Effects of Temperature Variations.

A variation of the cell temperature will produce a variation of the gas pressure within the cell in accordance with the relationship:

$$P V = R_o T$$

where P = gas pressure in newton/meter^3

V = volume of cell in meter^3

R_o = gas constant

= 8.317×10^3 joule/kg-mole °k

T = absolute temperature in °K

Temperature and pressure are not the only variables in the above relationship. Allowance must be made for the thermal expansion of the cell dimensions which results in a variation in volume.

The cells used in the measurements were made of high quality Corning 7740 pyrex which has a linear thermal expansion coefficient of 32×10^{-7} parts per °C.[16] The cells were in the form of right circular cylinders with outer diameters of two inches and heights of three inches.

The change in volume of the gas cell over the operating temperature range was found as:

$$V = \pi r_o^2 h_o \ (1 + .0000032 \ \Delta T)^3$$

$$= V_o \ (1 + .0000032 \ \Delta T)^3$$

where V = volume of the cell

r = radius

h = height

ΔT = temperature change in °C

The range of temperatures over which a satisfactory signal was obtained extended from 50°C to 75°C, the upper limit being the maximum temperature achievable with the experimental set-up. Thus, for a temperature change from one extreme to the other ($\Delta T = 25$°C)

$$V/V_o = (1.0000800)^3$$

$$= 1.000240019200512$$

Therefore, the change in volume due to the extreme temperature variation is not very significant, only 24 parts in 10^5, and is considered negligible.

Thus, the relationship becomes one where the buffer gas pressure is directly proportional to the absolute temperature:

$$P = k' T$$

Utilizing the above relationship, it is found that the temperature change of 25°C in the operating range represents a pressure change of 8.1% of the filling pressure. Due to the linearity of the above relationship, the temperature shift is best expressed for each buffer gas in the units of cycles per second per mm of Hg pressure - degree Centigrade. The predicted values of temperature shift were computed from the values of pressure shift listed in Table 3-1 and are listed in Table 5-1.

Table 5-1

Predicted Temperature Shifts

Buffer Gas	Shift (cps/mm of Hg-°C)
He	0.14
H_2	0.12
Ne	0.08
Ar	0
Kr	-0.15

Measurements of frequency versus temperature variations were conducted on cells containing helium at 49 mm of Hg and neon at 35 mm of Hg to verify the predictions of Table 5-1. The results obtained are listed in Table 5-2.

Table 5-2.

Measured Temperature Shifts

Buffer Gas	Shift (cps/mm of Hg-°C)
He	0.16 ± 0.10
Ne	0.07 ± 0.05

The accuracy of the temperature measurements was limited. The thermometer utilized had a very slow response. In addition, the cell mount, which was made of polyfoam, caused considerable thermal lag in the cell. It was necessary to withdraw the thermometer from the cavity in order to obtain a signal because the thermometer affected the cavity tuning. Therefore, the temperature measurements were very time-consuming which made possible errors due to temperature drift. For these reasons, a relatively large probable error was assigned in Table 5-2. When the probable errors were considered, the measured temperature shifts proved sufficiently close to the predicted values to support the theory leading to the predicted values.

The pressure shift measurements were made at a cell temperature of 67°C. In order to get the correct buffer gas pressure at the time of measurement, it was necessary to compute the pressure increase from the measured filling pressure. The temperature of the cell at the time that the pressure was measured at filling was approximately 35°C. The above change in temperature is equivalent to a pressure increase of 10.4 per cent.

6. Conclusion.

6-1. Summary of Results.

(1) The frequency shifts due to the pressures of various buffer gases were measured and recorded. The results of these measurements are plotted in Fig. 3-9 and recorded in tabular form in Table 3-1 on page 33.

(2) The effects of temperature variations upon the transition frequency were demonstrated to be proportional to the change in temperature, the pressure shift characteristic of the buffer gas and the buffer gas pressure.

(3) Wall-coated cells were shown to be free of temperature effects upon the transition frequency. The signal-to-noise ratio from the wall-coated cell was relatively strong and the line width attainable was moderately narrow.

(4) The hyperfine frequency of K^{39} was measured to be 461,719,785 $\pm$ 35 cps. The accuracy obtained from the optical pumping technique amounts to an increase of three more significant figures in the hyperfine frequency than was known previously.

6-2. Evaluation of Results.

For applications in frequency standards, the pressure shift is generally objectionable. Although the pressure shift affords some small amount of flexibility in the selection of a transition frequency, it makes the system temperature sensitive which lowers the system stability. For this reason, the results of the measurements made on the wall-coated cells are very promising.

The results of the pressure shift measurements using various buffer gases show pressure shifts can be predicted to a reasonable accuracy by knowledge of the hyperfine frequency under study and the pressure shifts for other hyperfine frequencies.

Of the buffer gases, argon stands out as having an extremely small pressure shift. With the exception of systems where the long-term stability requirement is greater than one part in 10^8, the use of argon at low pressure should prove quite satisfactory.

The technique applied to measure the transition frequency by counting a sub-multiple demonstrates flexibility of the optically pumped frequency standard. By proper selection of the alkali metal vapor and the sub-multiple, it is possible to develop a system for any number of frequencies, using a crystal oscillator and selected multiplier stages. The hyperfine frequencies for a few of the alkali metals are listed in the following table:

Table 6-1

Hyperfine Frequency

Alkali metal	Hyperfine frequency
K^{41}	254.018 mcs
K^{39}	461.720 "
H^{1}	1420.406 "
Na^{23}	1771.626 "
Rb^{87}	6834.683 "
Cs^{133}	9192.632 "

6-3. Possible Applications.

The major limitation of the optically pumped gas cell frequency standard system utilized in this project, as far as applications in electronic systems requiring stable frequency sources are concerned, is that the oscillator output frequency is frequency modulated. The center frequency of the output can be made very stable but applications for swept frequency outputs are very few. The swept frequency has served to provide the phase information necessary for servo control of the standard and to raise the signal-to-noise ratio.

A system utilizing two absorption cells with slightly different transition frequencies, each with a monitoring solar cell, will provide an output characterisitic identical in form to that of the synchronous amplifier when the solar cells are connected in series. The direct current output level of each solar cell will be dependent upon the signal generator frequency. The separation in transition frequencies of the two absorption cells can be attained through buffer gas pressure shifts. Temperature shifts can be cancelled out by selection of one buffer gas with a negative pressure shift characteristic and the other with a positive characteristic. Coupling the outputs of the solar cells to a differential amplifier would cancel out all first order effects due to lamp noise. Since the phase information would be present in the output characteristic, the frequency sweep would no longer be required.

A direct coupled amplifier channel in the above system is probably feasible although considerable engineering would be required. Any noise or change in system characteristics would be interpreted as a signal. The magnitude of the problem is foretold by the amount of gain required in the

amplifiers; i.e., approximately 500,000. However, by modulating the light beam at about 20 kcs and superimposing this signal on the photocurrent signal as a monitor of the amplifier noise and characteristics, a large amount of the noise could be cancelled using differential amplifier techniques.

The direct-coupled system is not the only approach to eliminate the need for the swept frequency. An a-c coupled channel would be possible by utilizing an interrupted signal at an audio rate. A large magnetic field inhomogeniety in the cell would cancel out any signal. Therefore, one method of obtaining an interrupted signal would be to feed a coil near the cell with a half-wave rectified signal.

6-4. Recommendations for Future Research.

In addition to considerations given the possible applications discussed in the previous section, future studies of the effects of buffer gases upon the hyperfine frequency of an alkali metal should note carefully the results obtained from mixtures of two or more buffer gases.

Also, a study of the improvement in signal obtained by the addition of a buffer gas to a wall-coated cell should prove interesting

BIBLIOGRAPHY

1. E. C. Beaty, P. L. Bender and A. R. Chi, Narrow Hyperfine Absorption Lines of Cs^{133} in Various Buffer Gases, Phys. Rev., 112, pp. 450-451, Oct. 15, 1958.

2. M. Arditi, The Principle of the Double Resonance Method Applied to Gas Cell Frequency Standards, ITTL Tech. Memo. 721, June 1958.

3. P. L. Bender, E. C. Beaty and A. R. Chi, Optical Detection of Narrow Rb^{87} Hyperfine Absorption Lines, Phys. Rev. Ltr., 1, pp. 311-313, Nov. 1, 1958.

4. M. Arditi and T. R. Carver, A Gas Cell "Atomic Clock" Using Optical Pumping and Optical Detection, ITTL Tech. Memo. 716, Mar. 1958.

5. W. Franzen and A. G. Emslie, Atomic Orientation by Optical Pumping, Phys. Rev., 108, pp. 1453-1459, Dec. 15, 1957.

6. W. E. Bell and A. L. Bloom, Optically Detected Field-Independent Transition in Sodium Vapor, Phys. Rev., 109, pp. 219-220, Jan. 1, 1958.

7. M. Arditi, An Evaluation of the Stability and Accuracy of a Breadboard Model of a Cesium Gas Cell Atomic Frequency Standard, ITTL Tech. Memo. 747, Jan. 1958.

8. J. P. Wittke and R. H. Dicke, Redetermination of the Hyperfine Splitting in the Ground State of Atomic Hydrogen, Phys. Rev., 103, pp. 620-624, Aug. 1956.

9. R. H. Dicke, The Effects of Collisions Upon the Doppler Width of Spectral Lines, Phys. Rev., 89, pp. 472-473, Jan. 15, 1953.

10. E. C. Beaty and P. L. Bender, Optical Detection of the Cesium Hyperfine Splitting, Bull. Amer. Phys. Soc., 3, pp. 185, May 1, 1958.

11. L. I. Schiff, Quantum Mechanics, McGraw-Hill, 1955.

12. P. Kusch and R. Taub, The g_J Values of the Alkali Atoms, Phys. Rev., 75, pp. 1477-1478, May 15, 1949.

13. H. C. Robinson, E. S. Ensberg and H. G. Dehmelt, Preservation of Spin State in Free Atom-Inert Surface Collisions, Bull. Amer. Phys. Soc., p. 9, Jan. 29, 1958.

14. W. Franzen, Study of the Spin Relaxation of Optically Aligned Rubidium Vapor, Rept. of the Ann Arbor Conference on Optical Pumping, Univ. of Mich., June 15-18, 1959.

15. R. E. Howig, Vapor Pressure Data for the More Common Elements, RCA Rev., 18, pp. 195-204, June 1957.

16. J. E. Heldman, Techniques of Glass Manipulation in Scientific Research, Prentice-Hall Inc., 1946.

APPENDIX I

BREIT-RABI FORMULA

The frequency dependence of the hyperfine transitions upon the magnetic field strength is given by the Breit-Rabi formula:

$$f(F,m) = f/8 - (\gamma_I/2\pi)\, H\, m \pm (f/2)\sqrt{1 + mx + x^2}$$

where f = hyperfine frequency = 461.7 mcs for K^{39}

= 198.7 cps/gauss

$$x = \frac{(-\mu_J/J + \mu_I/I)\, H}{W}$$

= .00606 H

H = ambient magnetic field in gauss

F = Hyperfine quantum number

m = Zeeman quantum number

The sign of the last term is positive for F = 2 and negative for F = 1.

Substituting F = 1, m = 0, and F = 2, m = 0, into the formula and subtracting, one obtains the formula that relates the dependence of the field independent transition upon the strength of the magnetic field.

$$f' = f\sqrt{1 + (.00606\ H)^2}$$

Utilizing the binominal series and disregarding all terms with exponents of four or greater as being insignificant, the formula becomes

$$f' = f\left[1 + \tfrac{1}{2}\,(.00606\ H)^2\right]$$

In the case of K^{39}, f = 461.7 mcs and the relation reduces to:

$$f' = f + 8477\ H^2$$

APPENDIX II

REENTRANT CAVITY DESIGN

A reentrant cavity is in the form of a right circular cylinder with a tuning stub projected along the axis of the cylinder. A cross-section of the cavity is shown in Fig. II-1.

In the figure, if the dimension δ is sufficiently small to introduce an appreciable capacitance at the end of the tuning stub, the reentrant cavity may be considered as a short length of coaxial line that is resonated by a large lumped capacitance at the end of the center conductor. This capacitance can be calculated from the gap spacing and area as:

$$C = 0.225\ \pi \rho_1^2 / \delta \quad \text{pf}$$

where the dimensions ρ_1 and δ are given in inches. Utilizing the formulas for the inductance per unit length of coaxial line and the capacitance per unit length between conductors, the formula for the resonant wavelength in terms of the cavity dimensions is found to be:[3]

$$\lambda_0 = 2\pi \left(\frac{\mu_0 \rho_1}{2\delta} \ln \frac{\rho_2}{\rho_1} \right)^{1/2}$$

The above formula neglects the additional capacity due to fringing effects at the end of the tuning stub and must be multiplied by a factor of the order of 1.25 to 1.75 in order to obtain the true wavelength.

[3] T. Moreno, Microwave Transmission Design Data, Dover Publications, Inc., 1948. pp. 227-229.

The dimensions of the cavity used in the pressure shift measurements were:

$$z_o = 7\tfrac{1}{4}"$$

$$\rho_1 = 3/4"$$

$$\rho_2 = 6\ 15/16"$$

$$\delta = \text{variable from 0 to 3"}$$

These dimensions produced a resonant range from 294 to 490 mcs.

The materials used in the construction of the cavity were:

(1) 20 guage sheet copper for the wall

(2) copper laminate sheets backed by 3/4" plywood for the ends.

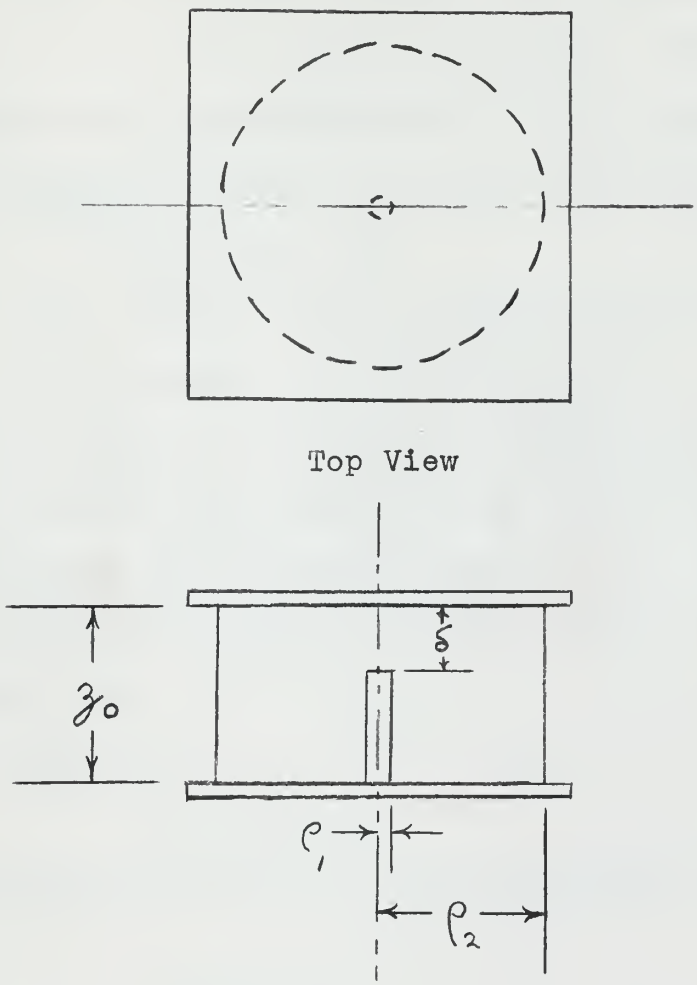

Figure II-1. Cross Section of Reentrant Cavity

APPENDIX III

FREQUENCY CORRECTION FOR AMBIENT MAGNETIC FIELD STRENGTH

The strength of the ambient magnetic field was determined by utilization of the gas cell magnetometer principle. The frequency of the transition between Zeeman sublevels is directly proportional to the strength of the ambient magnetic field and is given below:

(I) $$f_z = 700\ H \quad \text{kcs}$$

where f_z = Zeeman transition frequency in kcs

H = magnetic field strength in gauss

The transition frequency was determined by superimposing a radio frequency field whose frequency was varied about 350 kcs until a signal was obtained by the optical pumping technique. By this technique, the transition frequency was measured to be 357.1 kcs with a line width of approximately 3 kcs.

From formula (I):

$$H = 0.51 \text{ gauss}$$

Substituting this value of H into the Breit-Rabi formula:

$$f = 8477\ H^2$$

$$= 2205 \pm 3 \text{ cps}$$

To obtain the zero field hyperfine frequency, the above correction was subtracted from measured values of hyperfine frequencies.

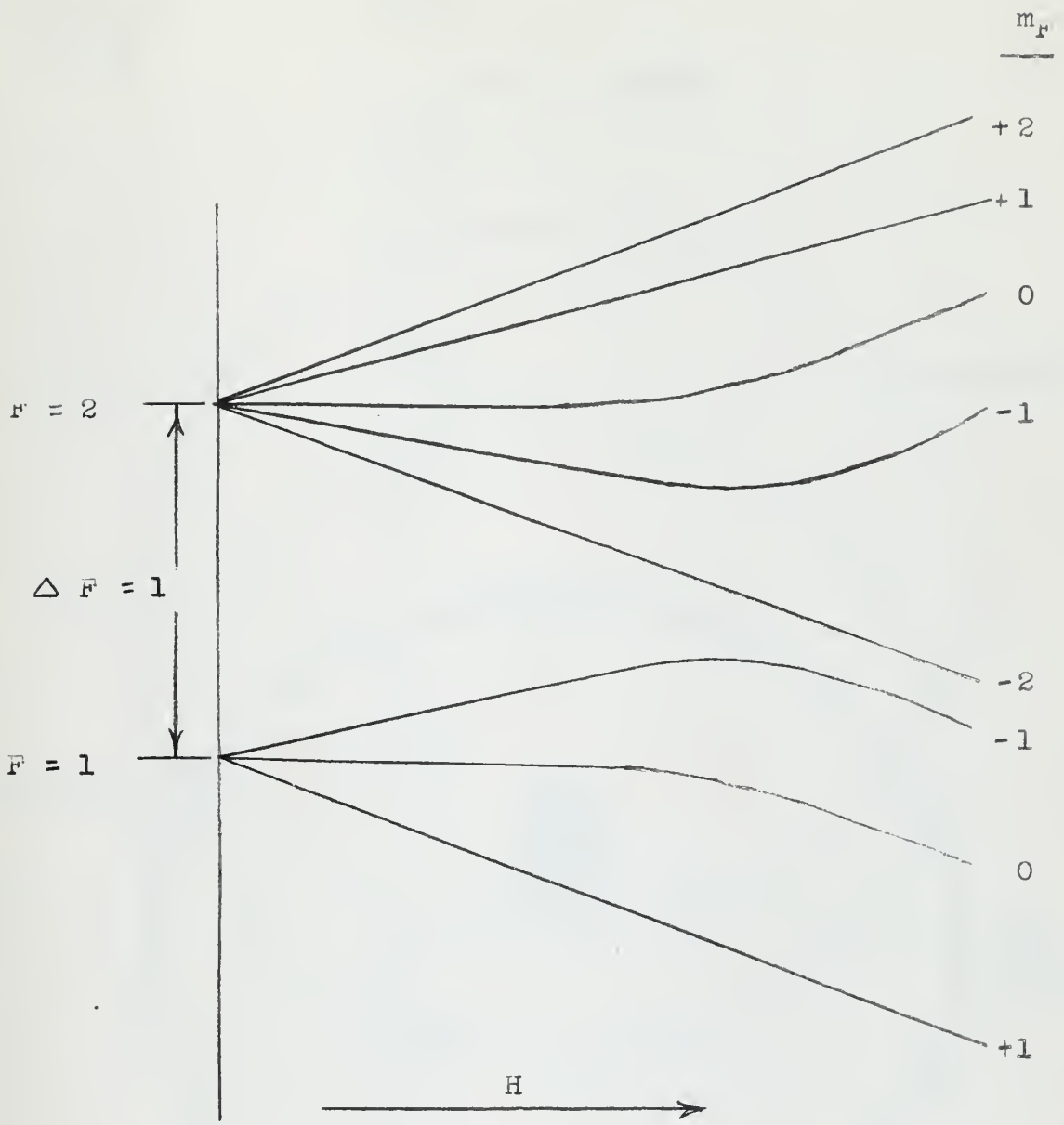

Figure 1-1. Energy Level Diagram of $4S_{\frac{1}{2}}$ Ground State of K^{39}

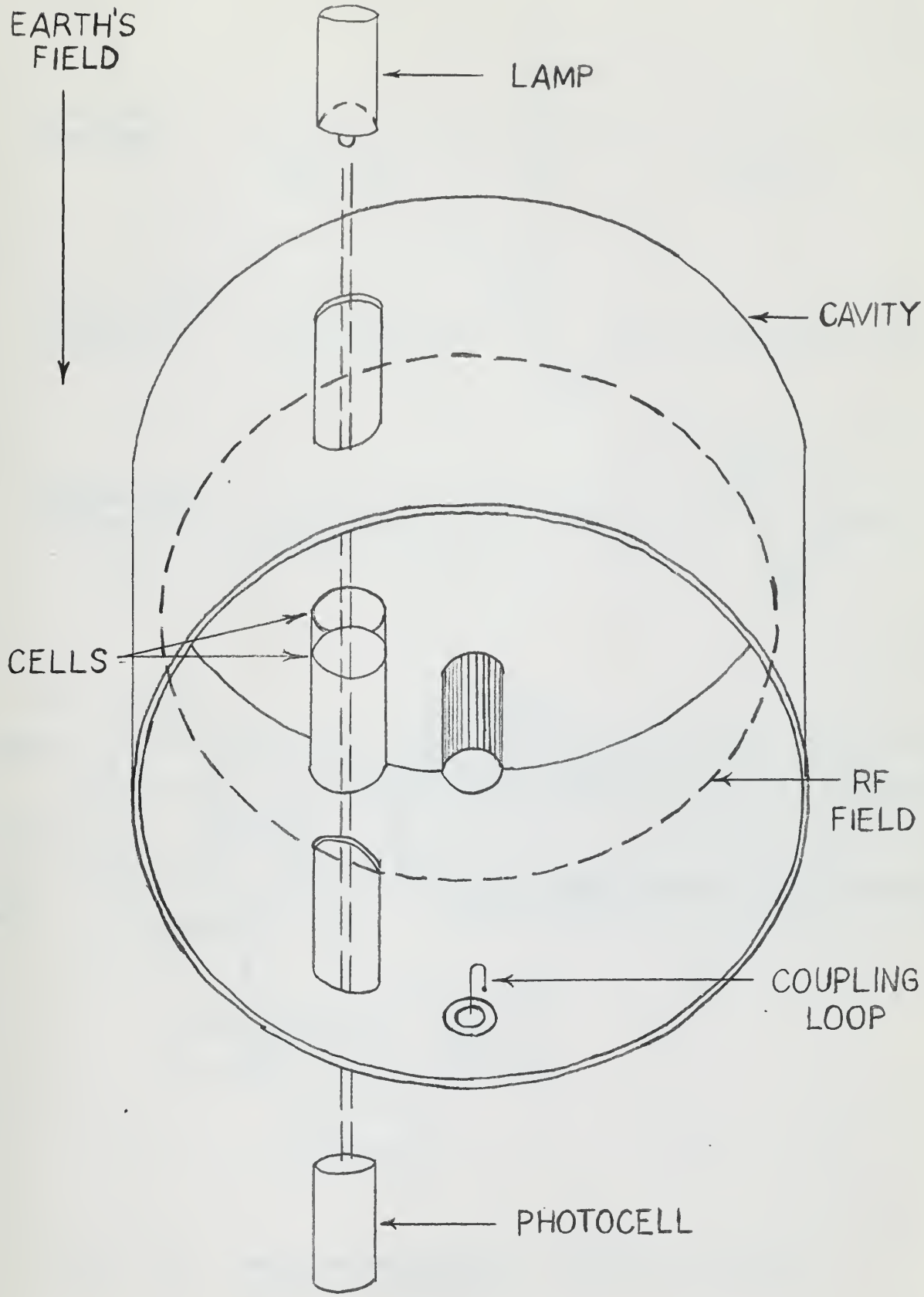

Figure 3-1. Sketch of Cavity and Optical Arrangement

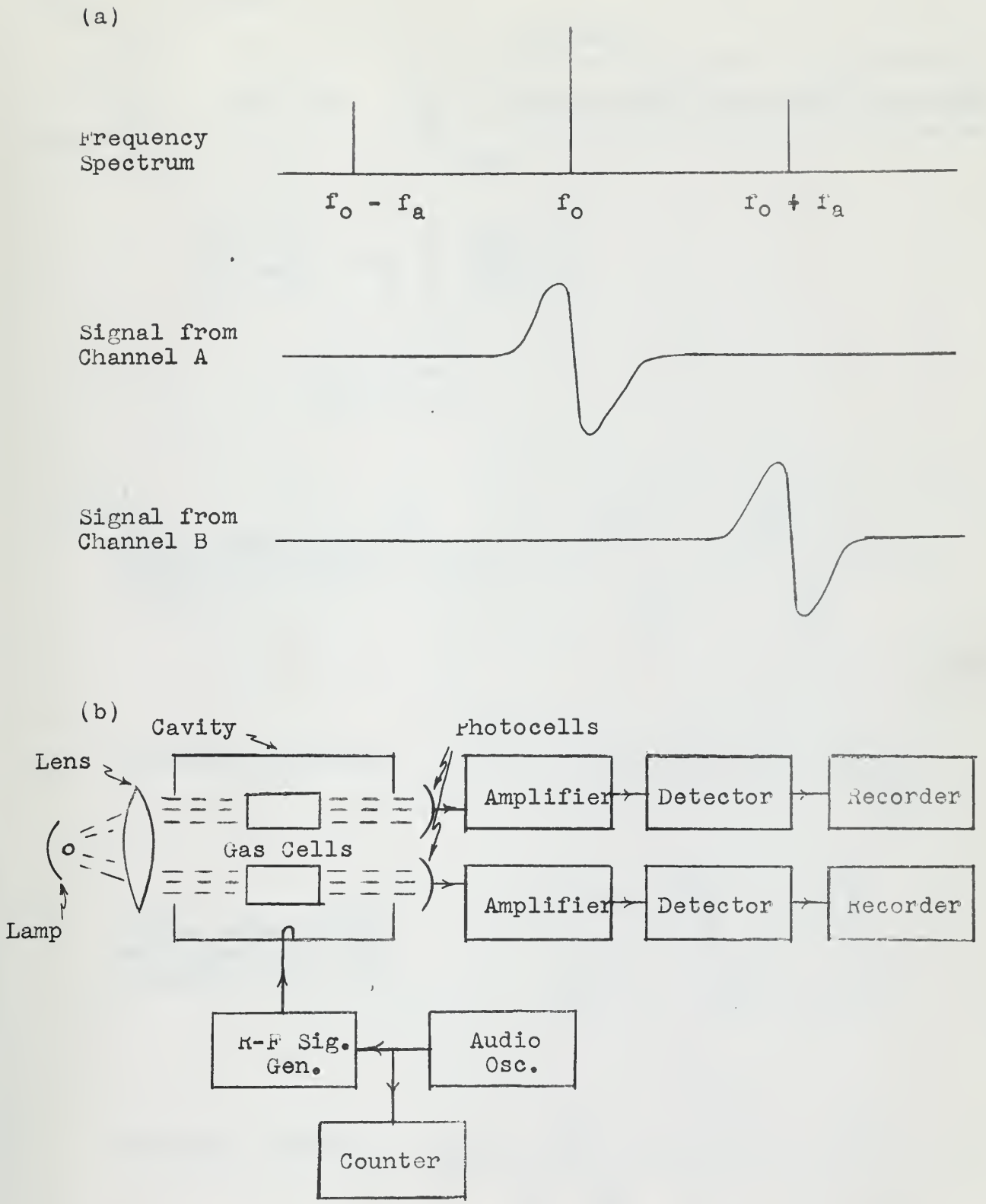

Figure 3-2. Proposed Measurement Technique Using Two Detection Channels

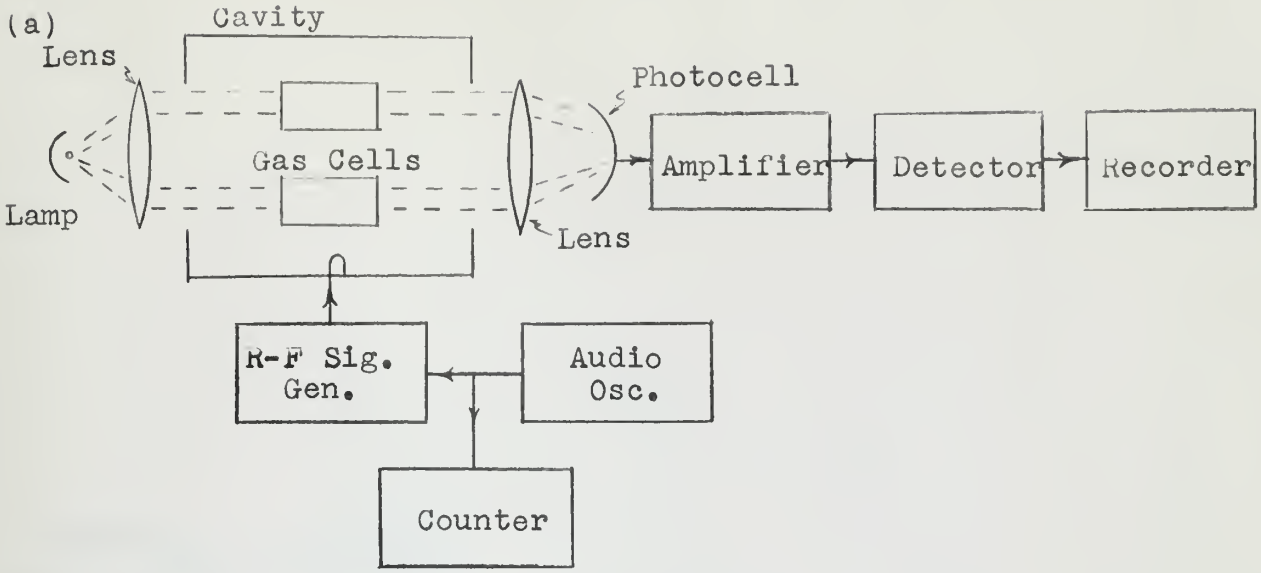

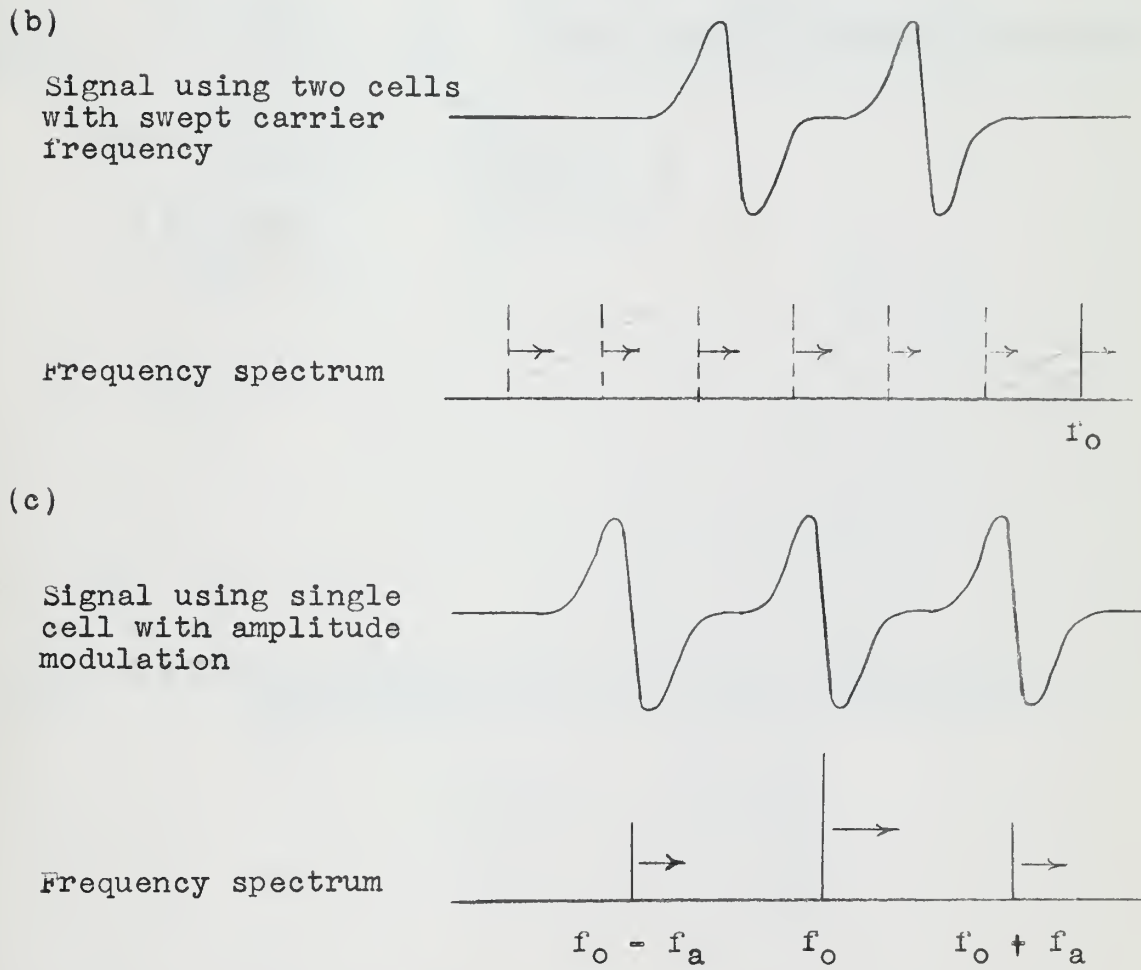

Figure 3-3. Proposed Measurement Technique Using Sideband Calibration

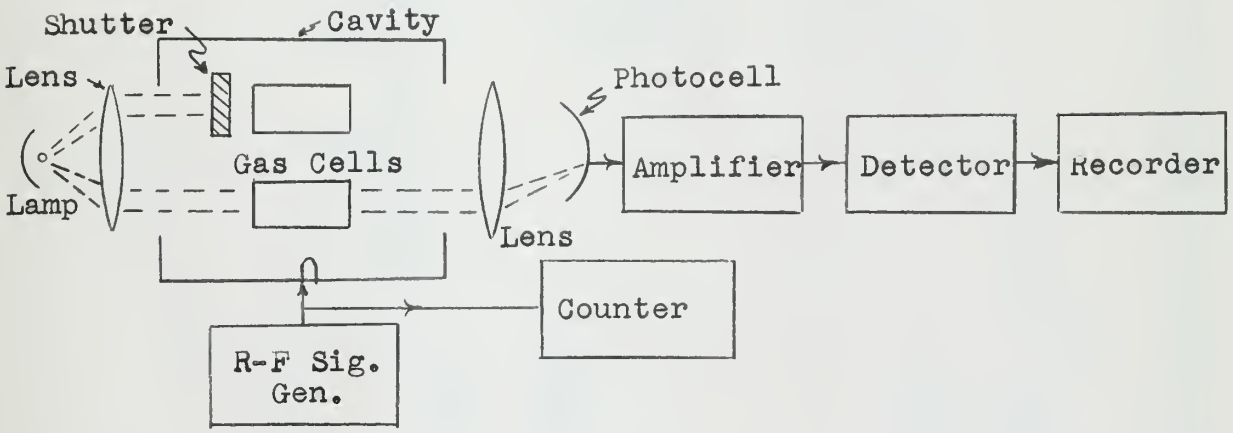

Figure 3-4. Proposed Measurement Technique Using Direct Measurement

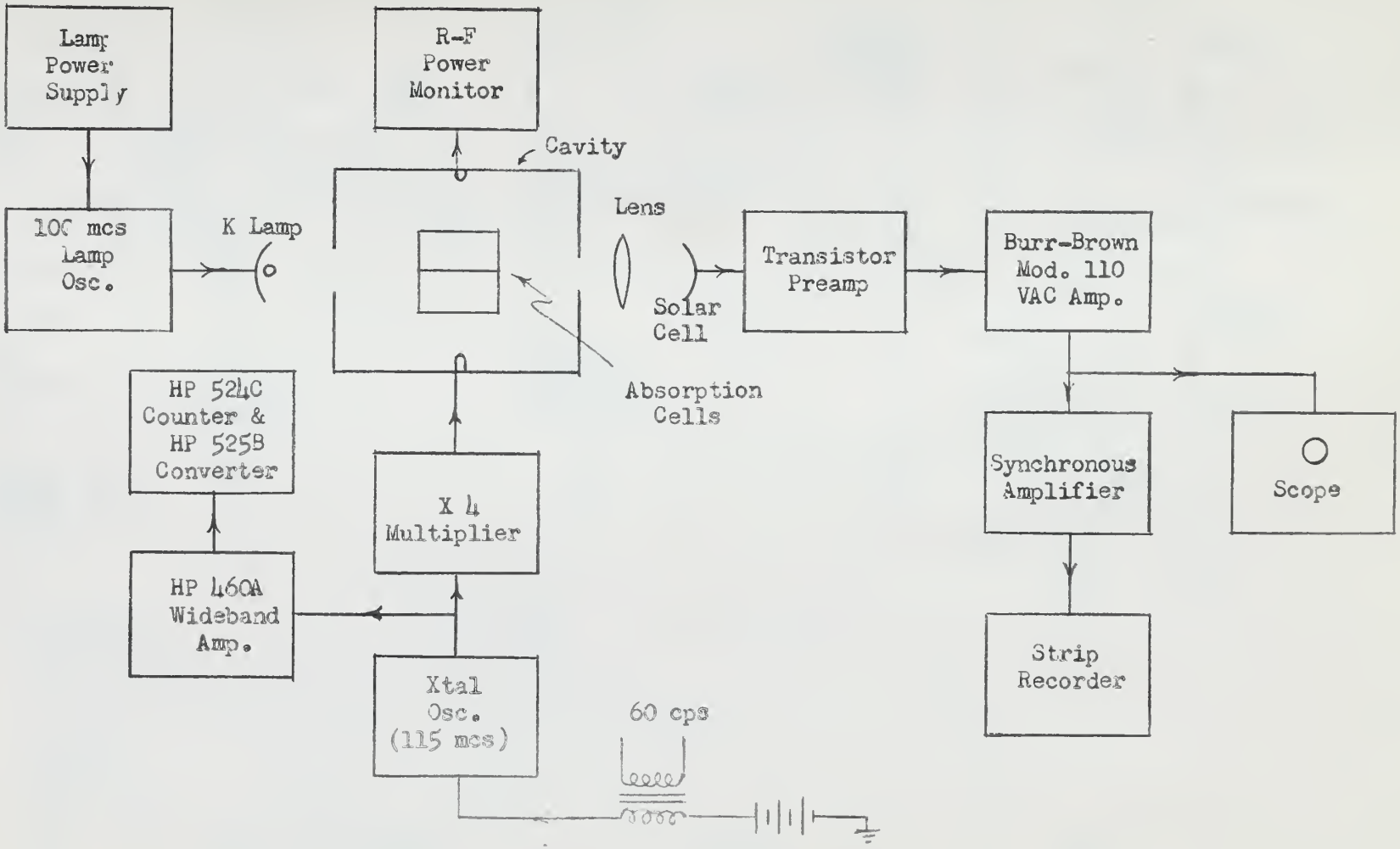

Figure 3-5. Block Diagram of Gas Cell Frequency Standard

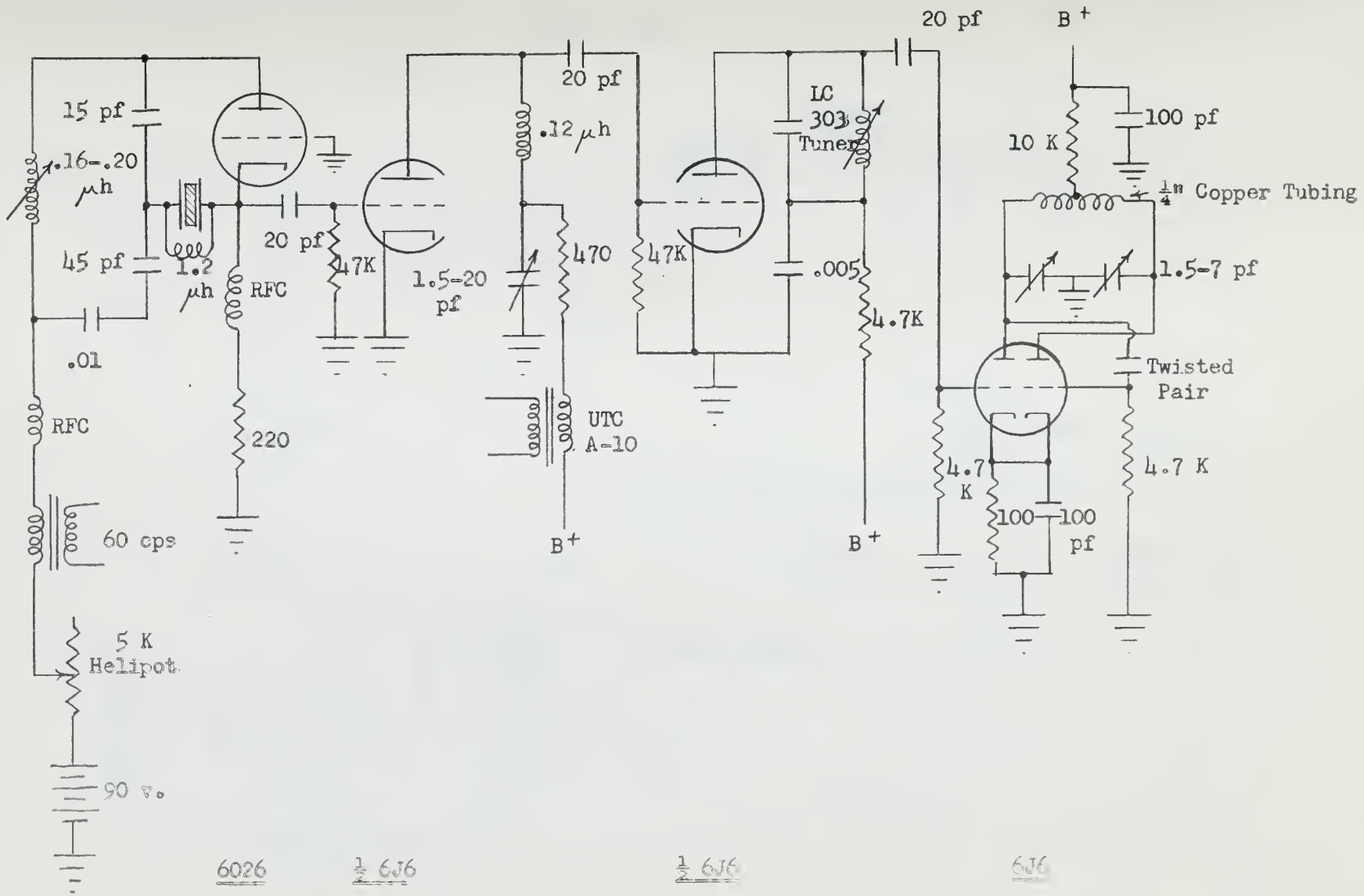

Figure 3-6. Schematic of 462 mcs. Crystal-controlled Radio Freque[illegible]

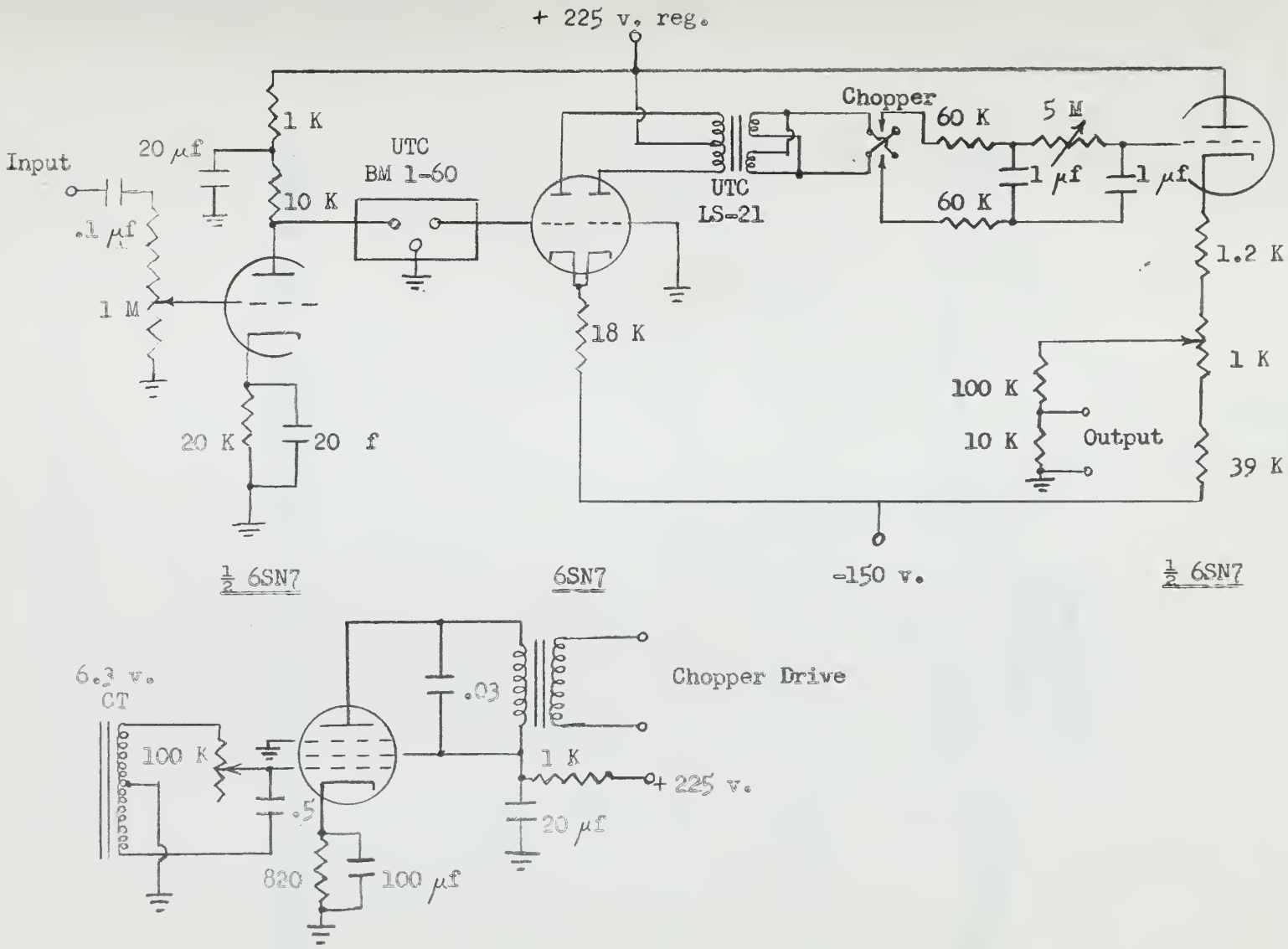

Figure 3-7. Schematic of 60 cps Synchronous Amplifier

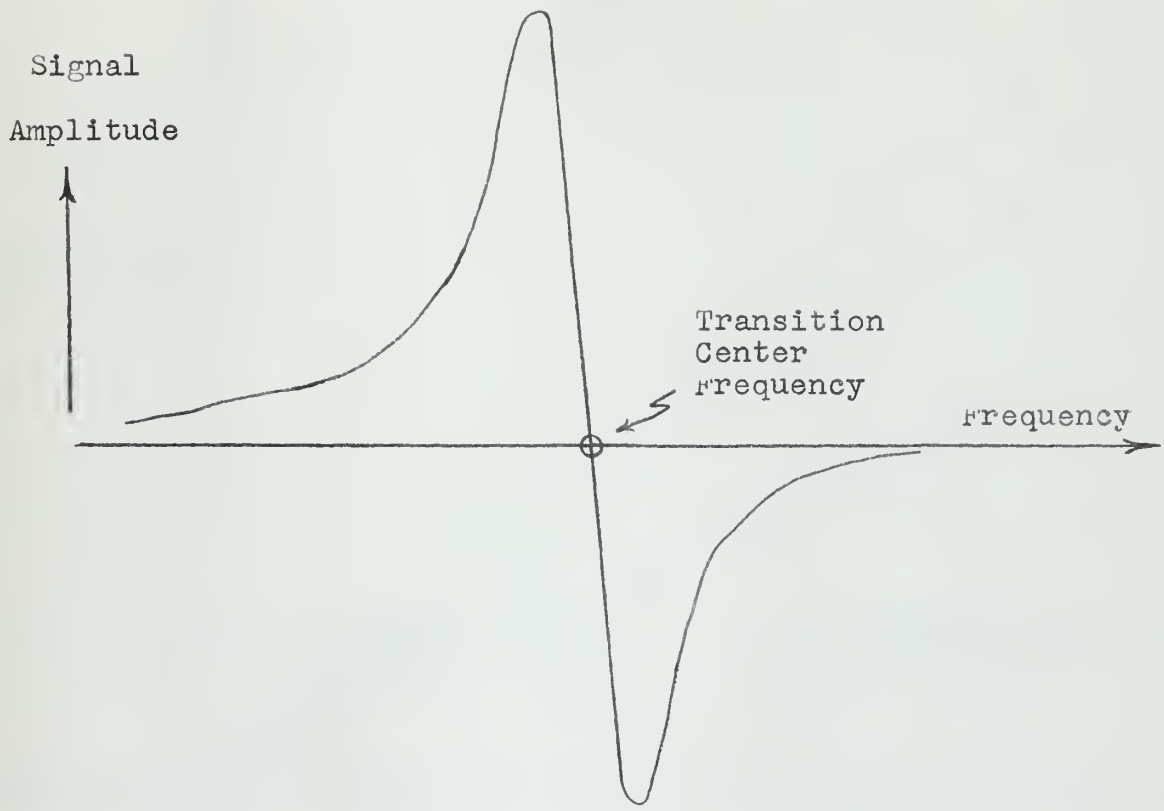

Figure 3-8. Output Signal of Synchronous Amplifier

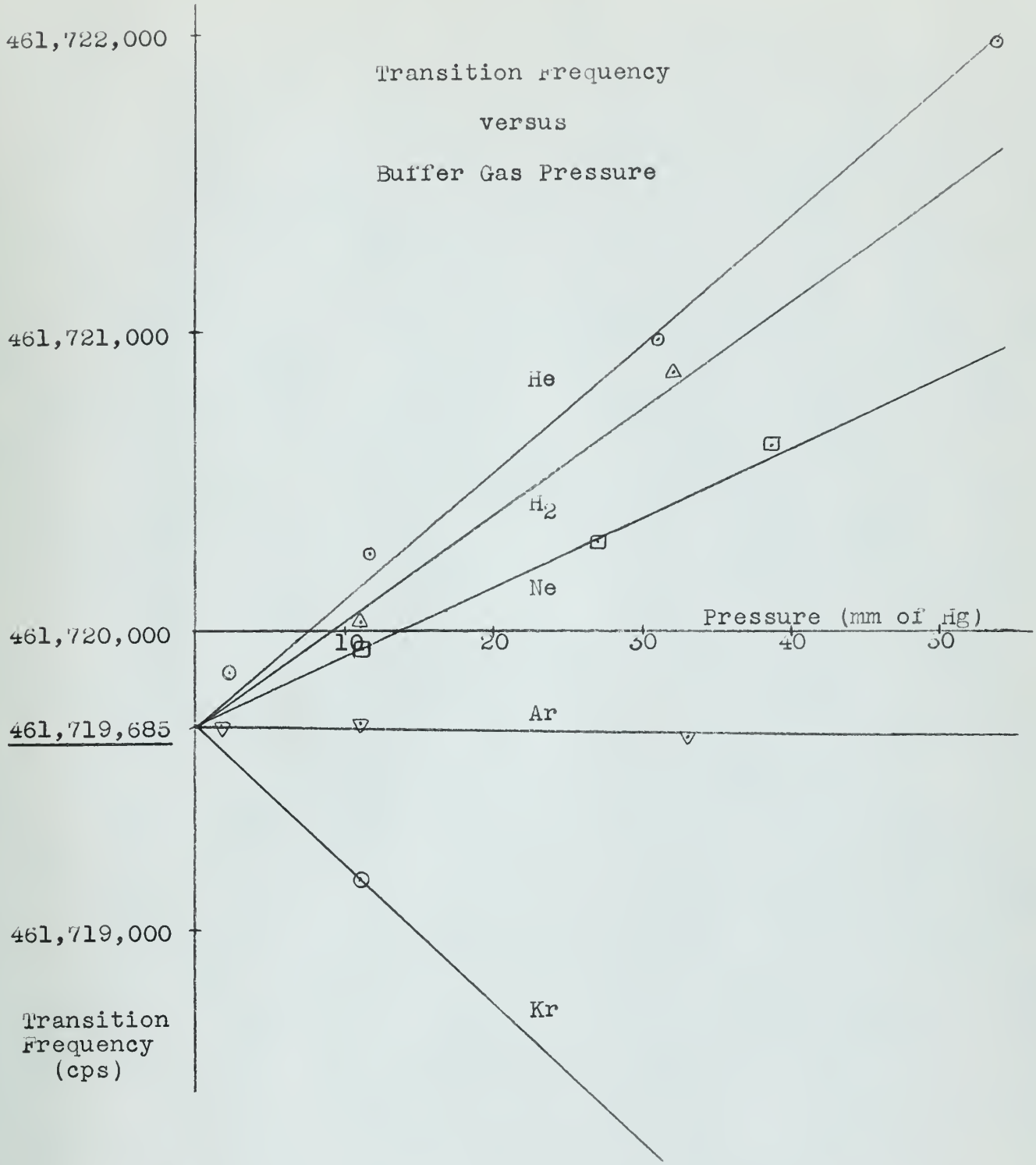

Figure 3-9. Buffer Gas Pressure Shifts in K^{39}